Influence of the inoculation process, the chemical composition and the cooling rate, on the solidification macro and microstructure of ductile iron

G.Rivera, R.Boeri and J.Sikora*

Metallurgy Division – INTEMA – Faculty of Engineering – National University of Mar del Plata – CONICET, Av. Juan B. Justo 4302, (B7608FDQ) Mar del Plata, ARGENTINA

The solidification structure of any casting has a marked influence on its final microstructure and properties. Nevertheless, the correlation between solidification structure, microstructure and properties has not been clearly established for ductile irons.

The objective of this investigation is to study the influence of the inoculation process, the chemical composition and the cooling rate on the solidification macro and microstructure of ductile irons cast in sand moulds.

The results show that primary and eutectic austenite always grow dendritically, even for hypereutectic alloys. The solidification macrostructure is characterised by the grain size and morphology of the austenite, revealed by using a special technique developed earlier by the authors. The solidification microstructure is characterised by a parameter related with the location of the microsegregated last to freeze regions.

Changes in the inoculation process do not cause significant modifications in the degree of the refinement of the solidification macro and microstructures. The carbon equivalent affects the grain size. The cooling rate, on the other hand, has a weak effect on the grain size and morphology, but strongly affects the dendrite arm spacing of the austenite.

Keywords: ductile iron, macrostructure, microstructure, inoculation, chemical composition, cooling rate

Introduction

As for most metallic alloys, the structure developed during solidification of ductile iron (DI) affects its room temperature microstructure, and as a result its mechanical properties. DI is customarily produced with near eutectic chemical composition. Its solidification involves the precipitation and growth of austenite and graphite spheroids from the melt. The growth of austenite and graphite continues until the liquid is exhausted, leading to a matrix formed by austenite that contains a dispersion of graphite spheroids. Nevertheless, upon cooling below the eutectoid temperature range, austenite usually transforms into different products, depending on the cooling rate and chemical composition, masking the original solidification structure. This makes it difficult to reveal that solidification structure. As a result, different explanations about the nature of the process of solidification of DI have been proposed over the years, and there is not a widely accepted one. The oldest explanation of the solidification of DI, still sustained by some researchers, proposes that the solidification unit of DI is formed by a single graphite nodule that is enveloped by a nearly spherical austenite layer, as shown schematically in Figure 1[1,2,3,4]. This will be referred to as the uni-nodular model's solidification unit. This view of the solidification led to the generalised believing that the degree of refinement of the solidification structure is directly related to the density of nodules in the matrix. As a result, standard characterisation of DI involves the identification of the nodule count and nodule size (ASTM A247). Significant research efforts have been focused on the development of technologies aimed to control the morphology, count, size and distribution of graphite nodules in DI. This has been achieved mainly by introducing careful controls of the chemical composition of the melt and by the development of proper spheroidisation and inoculation techniques.

The validity of the solidification mechanism proposed on Figure 1 has been often challenged. Some researchers have proposed that the solidification of eutectic DI involves the precipitation of austenite dendrites and graphite spheroids from the melt, leading to the formation of solidification units that contain several graphite spheroids, as show schematically in Figure 2[5,6]. This will be referred to as the multi-nodular model's solidification unit. In addition to the obvious difference in the number of nodules inside each solidification unit, both solidification models involve significant differences in the pattern of microsegregation produced during solidification, as a result of the differences in the distribution of the last to freeze portions of melt (LTF). These differences are shown schematically in Figures 1 and 2. The location of the LTF is represented by grey coloured areas. The distribution of LTF is coarser for the model that assumes dendritic growth of austenite. Therefore, after being solidified in similar conditions, the single nodule model would predict a more disperse microsegregation and therefore a more homogeneous microstructure, which could lead to better mechanical properties.

*Author for correspondence
e-mail: jsikora@fi.mdp.edu.ar

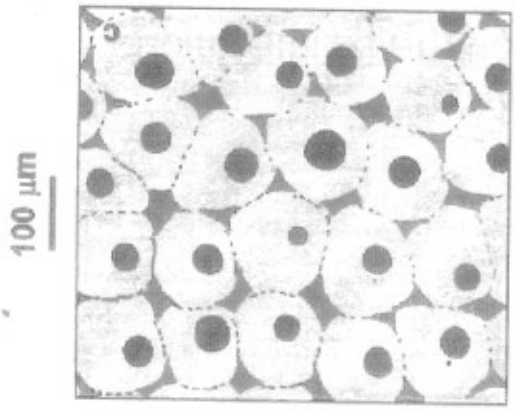

Fig.1 Solidification structure according to uni-nodular model. Black dotted lines represent the solidification unit boundaries

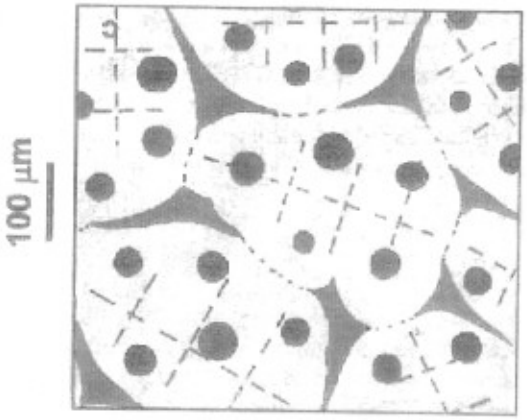

Fig. 2 Solidification structure according to multi-nodular model. Black dotted lines represent the solidification unit boundaries. Dashed lines show dendrite axes

The results of other studies about the nucleation and growth of austenite in DI have further increased the controversy about the subject. Patterson and Dopp[7], describe the existence of two types of austenite dendrites, exogenous and endogenous, depending on the cooling condition prevailing at a given location of a casting. Ruff and Wallace[8] analysed the effect of the inoculants on the nucleation and growth of primary austenite, and reported that nitrides, carbonitrides and carbides present in the melt, act as substrates for austenite nucleation, and that the number of austenite dendrites can be increased by reducing the equivalent carbon content. Mampaey and Xu[9] relate the size and the orientation of austenite dendrites with the heat flow, and show that dendrites nucleate at the mould walls. They also report that two types of austenite were identified by using colour metallography, primary and eutectic austenite dendrites. Miyake and Okada[10] studied the change in the characteristics of the primary austenite for different process modifications, aiming to identify its influence on the nucleation and growth of eutectic austenite. They found that as the cooling rate increases, the primary austenite morphology changes from endogenous to exogenous. Dioszegi et al[11] propose that two types of austenite can be found in hypoeutectic grey irons, a dendritic primary austenite, and a eutectic austenite that grows at the interdentritic regions of primary austenite. A common problem that troubles most investigations is the difficulty to reveal the solidification structure.

Recently, the authors developed new techniques to reveal and to characterise the micro and macrostructure of DI[12,13]. Through these techniques, the authors obtained new evidences that led them to propose that the solidification of eutectic DI takes place as shown schematically in Figure 3[12,13]. According to this model, the solidification starts with the independent nucleation of austenite and graphite from the melt. The growth of austenite is dendritic, as shown in Figures 3-a and 3-e. As the solid fraction increases, the austenite dendrites collide with most graphite particles and envelop them. Further growth of the graphite is controlled by the diffusion of C from the melt to the graphite, through the austenite envelope. As each dendrite grows, it retains a large volume fraction of melt between its secondary arms. Indeed, at the time the dendrites impinge on each other, defining the grain size, a large volume fraction of liquid remains inside each grain. The final structure is represented in Figures 3-c and 3-g. Figure 3-c shows the relatively coarse grained structure. Figure 3-g shows the LTF regions in dark grey. According to the proposed evolution of the morphology of the solid phases during solidification, the last melt to freeze lies between secondary dendrite arms. This means that a large number of isolated liquid pockets are located inside each grain before solidification ends. The LTF are then intragranular. The dark grey dotted lines, manually drawn between the locations of neighbouring LTF regions, define the closed regions called "cells"[13].

The authors have also studied the solid state transformations of DI and the influence of the microsegregation on them[14,15,16,17].

The objective of this investigation is to apply the newly developed techniques, in order to identify the influence of the inoculation process, the chemical composition and the cooling rate on the solidification micro and macrostructure of DI.

Experimental methods

The DI melts were produced in a 60Kg induction melting unit. The melts were nodularised by using 2 wt% of Fe-Si-Mg-Ca-Ce (9%Mg) and inoculated with 0.65wt% of FeSi(75%), using the sandwich method. The melts were poured into cylindrical resin bonded silica sand moulds. The chemical composition of the melts and the diameter of the samples cast, are listed on Table 1. The cooling curves of some of these castings were recorded by using thermocouples located at their geometric centre, in order to measure the solidification time.

The melts I-1 and I-2, Table 1, that have nearly eutectic chemical composition, were made from the same base liquid iron, but using different inoculation

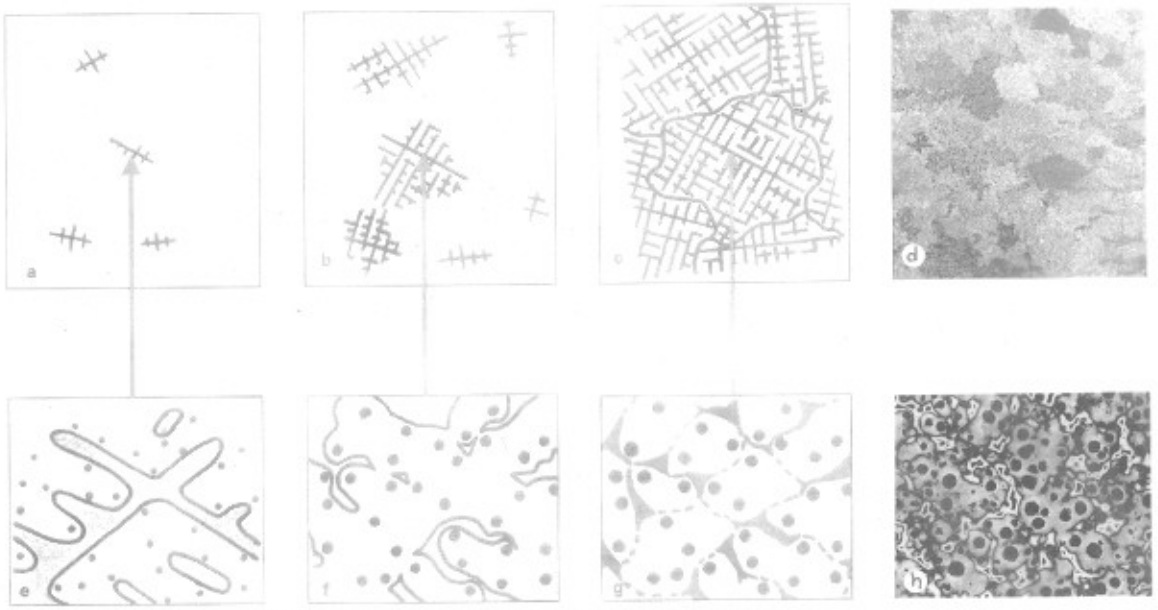

Fig. 3 Schematic illustration of the secuence of solidification of eutectic DI.
(a-c) solidification macrostructure (equiaxed grains); (d) actual macrostructure; (e-g) solidification microstructure; (h) actual microstructure [13]

Table 1 Chemical composition of the melts and diameter of the round bars in each case

Melt		Casting Diameter [mm]	Chemical composition [wt%]						
			CE	C	Si	Mn	Cu	Ni	Mg
I-1		20	4.16	3.26	2.71	0.22	0.35	0.33	0.048
I-2	$I\text{-}2_{T1}$	20	4.20	3.26	2.82	0.22	0.35	0.33	0.045
	$I\text{-}2_{T2}$	20							
C-1		20	3.99	3.06	2.79	0.34	0.61	0.62	0.050
		30							
		46							
C-2		20	4.26	3.35	2.75	0.36	0.63	0.60	0.046
		30							
		46							
C-3		20	4.70	3.61	3.27	0.33	0.63	0.59	0.051
		30							
		46							

procedure. Melt I-1 was nodularised and inoculated as stated above. Melt I-2 was additionally pos-inoculated in mould, using two methods. Melt $I\text{-}2_{T1}$ was inoculated by forcing the melt to pass through a hole drilled into a Tenbloc™ inoculating pellet, as shown schematically in Figure 4. Melt $I\text{-}2_{T2}$ was inoculated by locating a Tenbloc™ inoculating pellet at the running of a sand mould that acted as a mixing chamber.

The solidification structure of the samples was revealed by using two techniques developed earlier. The solidification macrostructure was revealed by applying the DAAS technique[17]. This technique requires to carry out a complex procedure which involves hot shake out and austempering of the cast parts. The objective is to produce the austempering of the DI starting from the austenite precipitated during solidification, which has the original grain crystalline structure. After austempering, a large proportion of such austenite is retained at the room temperature microstructure, allowing the observation of the macrostructure after etching with Picral(4%). DAAS was applied on the 20mm diameter round bars of melt I-1 and I-2, and on the 20, 30 and 46mm diameter round bars of melts C-1, C-2 y C-3.

The solidification microstructure was revealed by using a colour metallography technique that creates colour patterns that follow the microsegregation map[18]. Figure 5 shows the location of LTF regions, as revealed by colour metallography.

After samples are colour etched, they are photographed. The neighbouring LTF regions are manually connected by lines drawn on the photos. This procedure defines closed regions that are usually referred to as "cells", as shown in Figure 6. At least 50 cells were

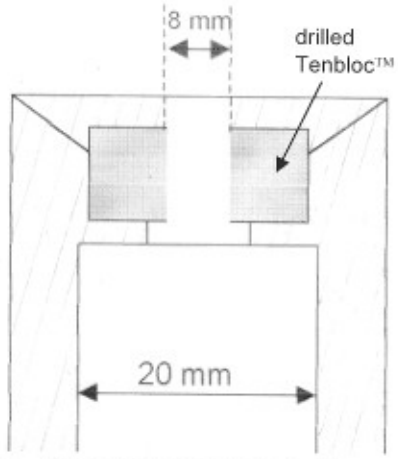

Fig. 4 Schematic of the pos-inoculation process for melt **I-2$_{T1}$**

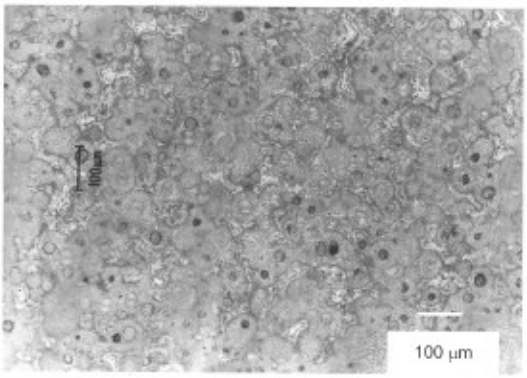

Fig. 5 Black and white print of a sample after colour etching

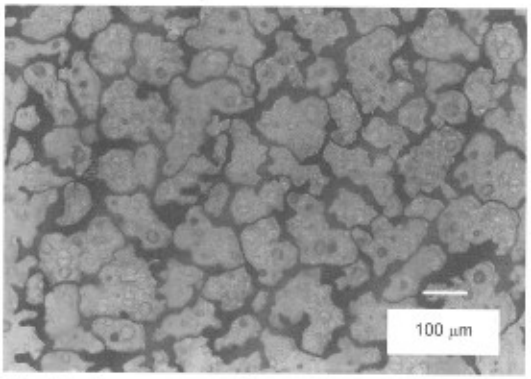

Fig. 6 Same area as Fig. 5. Cell contour marked manually

identified on each sample analysed, and the average number of cells per unit area (Nc) was calculated[13].

Results and Discussion

Influence of the inoculation on the solidification macro and microstructure

Table 2 lists values of nodule count (Nn) and count of grains per unit area (N_{grain}) for the 20mm diameter round bars of melts I-1, I-2$_{T1}$ and I-2$_{T2}$. The results show that in spite that the nodule count has increased in approximately 74% as a result of pos-inoculation, the grain size is similar among all samples. This suggests that, on castings of similar chemical composition and solidified at the same rate, a noticeable change in nodule count does not induce a significant change in the solidification macrostructure.

The influence of the inoculation on the solidification microstructure was analysed by colour etching samples of melts I-1 and I-2. Table 2 lists the values of cell counts (Nc) measured after etching. The results show that, comparing melts I-1 and I-2$_{T2}$, an increase in nodule count of 45% is accompanied by an increase of only 16% in the cell count. Similarly, comparing melts I-1 and I-2$_{T1}$, an increase of 74% in nodule count is accompanied by an increase of only 24% in cell count. These results lead to conclude that, for melts of similar composition solidified at the same rate, an increase in nodule count obtained by means of improved inoculation techniques, is not accompanied by a proportional refinement of the austenite structure. This contradicts the results of a number of studies[19,20,21,22] and suggests that increasing the nodule count is not an effective method to refine the solidification microstructure.

Table 2 Characterisation of the solidification micro and macrostructures

Melt	Nn [nod/mm^2]	N_{grain} [grains/mm^2]	Nc [Cell/mm^2]
I-1	301	3.08	50
I-2$_{T2}$	435	2.85	58
I-2$_{T1}$	524	2.92	62

Influence of the carbon equivalent on the solidification macro and microstructure

The influence of the carbon equivalent (CE) on the macrostructure can be assessed by comparing the grain count of castings solidified at the same rate, having different chemical composition. These values are listed on Table 3. Figure 7 shows the macrostructure of the 30mm round bars of melts C-1, C-2 and C-3. An equiaxed grained structure is clearly visible in all cases. Hypoeutectic melt C-1 shows larger grain size than eutectic melt C-2 and hypereutectic melt C-3. Grain size values measured are significantly smaller than those reported earlier by Boeri and Sikora[17], nevertheless the change in grain size as a function of carbon equivalent is coincident.

The effect of CE on grain size can be explained as follows. For hypoeutectic DI, cooling of the melt causes the nucleation of austenite at temperatures above the eutectic range. The number of heterogeneous nucleation sites for austenite is relatively small at this temperature. As austenite grows, it rejects carbon to the surrounding liquid, but the liquid far from the nucleus is not saturated in C. As a result, the growth of austenite becomes unstable, and growing nuclei develop dendritic shape. The growth of austenite is fast and takes place with negligible kinetic undercooling, conforming lean dendrites, that then grow relatively long distances until they impinge on other dendrites, defining a relatively

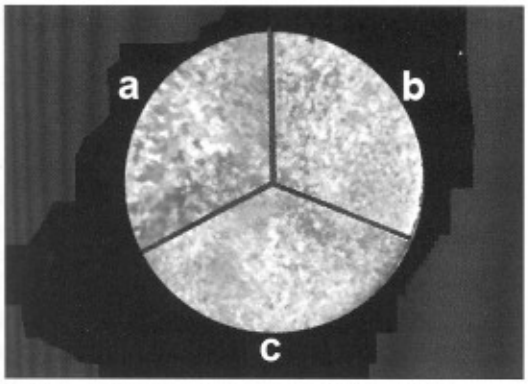

Fig. 7 Macrostructure of 30 mm round bars (a) melt C-1; (b) melt C-2; (c) melt C-3

large grain size. As the carbon equivalent increases and approaches eutectic concentration, the solidification of austenite starts at lower temperature. Heterogeneous nucleation of austenite may take place at precipitates of different nature, including graphite particles. The density of precipitates of such nature will be larger as the temperature decreases. Therefore, austenite nucleation will take place at a faster rate and the resulting grain size will be smaller. In any event, the growth of austenite dendrites seem to define the grain size. The completion of solidification will involve the solidification of the intradendritic melt. It is apparent that this event does not involve the nucleation of new austenite, but proceeds by the growth of the austenite dendrite arms, and the nucleation and growth of graphite at the intradendritic melt.

The influence of the CE on the solidification microstructure can be assessed by comparing the colour etched samples of castings solidified at the same rate, but having different chemical composition. Figures 8 and 9 show the microstructure of 46mm round bars of melts C-3 and C-1 after colour etching. It is clear that the pattern of microsegregation is very similar for both samples, even though one is hypereutectic and the other hypoeutectic. This observation is further supported by the results of Table 3, that show that cell counts are very similar for round bars of the same size, regardless their CE. Taking into account that the distribution of microsegregated regions is a direct consequence of the morphology taken by the solid phases during solidification, the results suggest that the solidification proceeds in a similar manner, regardless the CE value of DI. It is proposed that the mechanism of solidification of eutectic ductile iron presented earlier by the authors[12,13,17] can be extended to hypo and hypereutectic ductile irons. The results also support that even for hypereutectic ductile irons the austenite grows dendritically.

Influence of the cooling rate on the solidification macro and microstructure

Other aspect that needs to be analysed is the influence of the cooling rate on the solidification structure. The cooling curves showed that the solidification time of the 20, 30 and 46mm diameter round bars are approximately 50, 115, and 260 seconds, respectively. Figure 10 shows

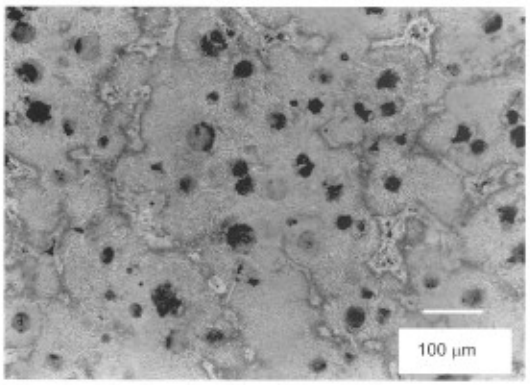

Fig. 8 Black and white print of melt C-3 colour etched

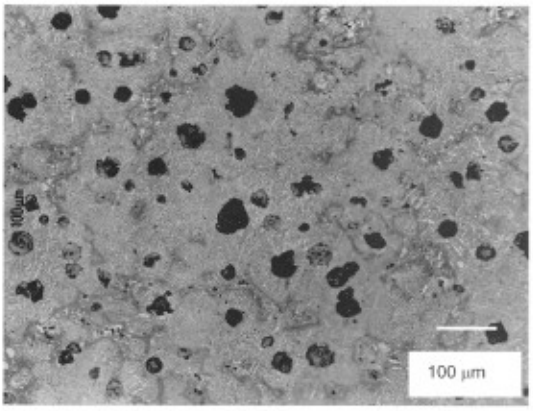

Fig. 9 Black and white print of melt C-1 colour etched

Table 3 Characterisation of the solidification micro and macrostructure

Melt	Diameter [mm]	Nn [Nod/mm^2]	N_{grain} [grains/mm^2]	Nc [Cell/mm^2]
C-1	20	231	1.58	41
	30	156	1.66	24
	46	110	1.64	14
C-2	20	256	4.16	42
	30	171	4.00	23
	46	123	3.57	15
C-3	20	296	4.54	42
	30	185	4.00	22
	46	132	3.70	15

the macrostructure of the round bars of 20 and 46 mm diameter of melts C-3 and C-1. It is remarkable that within the range of variations of solidification rates investigated, the grain size remains approximately constant, regardless casting size, as shown in Table 3. These results disagree with earlier reports[17] of the authors, which showed changes in the grain size as a function of the casting size, and also showed columnar grains at the sand cast round bars. The cause of this disagreement is uncertain.

The change in the solidification microstructure as the cooling rate diminishes can be assessed based on the values of Nc and Nn listed in Table 3. As the

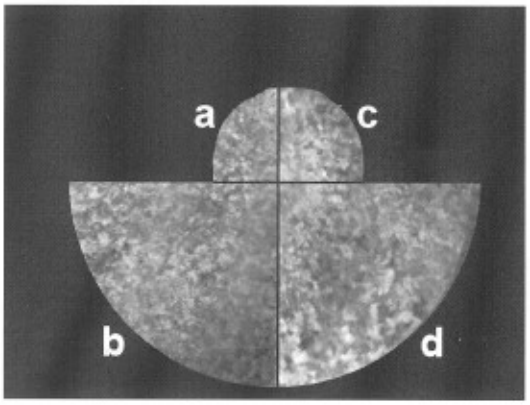

Fig. 10 Macrostructure of round bars
(a) 20 mm melt C-3, (b) 46 mm melt C-3
(c) 20 mm melt C-1, (d) 46 mm melt C-1

solidification rate decreases, both the solidification microstructure, characterised by Nc, and the graphite dispersion, characterised by Nn, become coarser.

Conclusions

- An increase in the nodule count of DI obtained through modifications in the inoculation procedure does not affect the macrostructure of eutectic DI.
- Increasing nodule count in approximately 70 %, only causes a small refinement of the solidification microstructure.
- Equivalent carbon content affects DI macrostructure. Hypoeutectic alloys show larger austenite grain size than eutectic and hypereutectic DI.
- The cooling rate during solidification did not affect markedly the macrostructure of DI within the ranges investigated. This was the case for hypo, hyper and eutectic irons.
- Faster cooling rates during solidification cause refinement of DI solidification microstructure, as made evident by the observation of finer distributions of the microsegregation and higher nodule counts.

References

1.E.Fraś, W.Kapturkiewicz and A. Burbielko, "Computer modelling of primary structure formation in ductile iron", Physical Metallurgy of Cast Iron V, *Advanced Materials Research*, 1997,Vol. 4-5,pp. 499-504

2. Ch. Charbon and M. Rappaz "3D stochastic modelling of nodular cast iron solidification", Physical Metallurgy of Cast Iron V, *Advanced Materials Research*, 1997, Vol. 4-5, pp. 453-460

3. J.Liu and R.Elliott, "The influence of cast structure on the austempering of ductile iron. Part 2:Assessment of model calculations of microsegregation", *Int. J. of Cast Metals Research*, 1999,Vol. 12, pp 75-82

4. B.Liu, "Progress in solidification modeling of cast iron in China", *Int. J. of Cast Metals Res.*,1999,Vol. 11, pp. 259- 266

5. R. Boeri and F. Weinberg, "Microsegregation in ductile iron", *AFS Transactions*, 1989, pp. 179-184

6. D. Banerjee and D. Stefanescu, "Structural transitions and solidification kinetics of SG cast iron during directional solidification experiments", *AFS Transactions*, 1991, pp.747-759

7. W.Patterson and R.Döpp, *Giesserei* 16, 1964,pp.49-86

8. G. Ruff and J. Wallace, "Control of graphite structure and its effect on mechanical properties", *AFS Transactions*, 1976, pp. 705-728

9. F. Mampaey and Z. Xu, 62nd World Foundry Congress

10. H. Miyake and A. Okada, "Nucleation and growth of primary austenite in hypoeutectic cast iron", *AFS Transactions*, 1998, pp 581-587

11.A. Dioszegi, A. Millberg and I.L. Svensson. The Science of Casting and Solidification. (Edited by D.Stefanescu, R. Ruxanda, M.Tierean and C. Serban, Rumania 2001) pp 269-277

12.J.Sikora, R.Boeri and G.Rivera.The Science of Casting and Solidification. (Edited by D.Stefanescu, R.Ruxanda, M.Tierean and C.Serban, Rumania2001) pp 321-329

13. G. Rivera, R. Boeri and J. Sikora, "Revealing and characterising solidification structure of ductile cast iron", *Materials Science and Technology*, 2002. In press

14. J. Sikora and R. Boeri, "Solid State Transformations in Ductile Iron - Influence of Prior Austenite Matrix Microstructure", *Int. J. of Cast Metals Research*, 1999, vol. 11, pp 419-424

15. J. Massone, R. Boeri and J. Sikora, "Production of ADI by Hot Shake Out – Microstructure and Mechanical Properties", *Int. J. of Cast Metals Research*, 1999, vol. 11, pp 419-424

16. I. Galarreta, R. Boeri and J. Sikora, "Free Ferrite in Pearlitic Ductile Iron – Morphology and its Influence on Mechanical Properties", *Int. J. of Cast Metals Research*, 1997, vol. 9, pp 353-358

17. R. Boeri and J. Sikora, "Solidification Macrostructure of Spheroidal Graphite Cast Iron, *Int. J. of Cast Metals Research*, 2001, Vol 13, pp 307-313

18. G.Rivera, R.Boeri and J.Sikora "Revealing the solidification structure of nodular iron", *Cast Metals*, 1995, vol.8, pp. 1-5.

19. A. Javaid and C.Loper, "Production of heavy-section ductile cast irons", *AFS Transactions*, 1995, pp. 135-150

20. C.Loper and R.Gundlach, "Inoculation, what is it and how does inoculation work?" (Int. Inoculation Conf. Proceedings, AFS, Illinois1998)

21. J.Liu and R.Elliott, "The influence of cast structure on the austempering of ductile iron. Part 1: Modelling of the influence of nodule count on microsegregation", *Int. J. of Cast Metals Research*, 1998, Vol. 10, pp.301-305

22.J.Lacaze, M.Castro, N.Aichoun and G.Lesoult, "Influence de la vitesse de refroidissement sur la microstructure et la cinétique de solidification de fontes G.S. expérience et simulation numérique de solidifiction dirigée", Mémoires et Etudes Scientifiques *Revue de Métallurgie*, 1989, pp 85-97